ISSN 1674-1056
http://cpb.iphy.ac.cn
http://iopscience.iop.org/cpb
中国物理 B
Chinese Physics
中国物理 Chinese Physics B

The upper bound function of nonadiabatic dynamics in parametric driving quantum systems

Lin Zhang(张林), Junpeng Liu(刘军鹏)

Citation: Chin. Phys. B . 2019, 28(8): 080301 . **doi:** 10.1088/1674-1056/28/8/080301
Journal homepage: http://cpb.iphy.ac.cn; http://iopscience.iop.org/cpb

What follows is a list of articles you may be interested in

Gazeau-Klauder coherent states examined from the viewpoint of diagonal ordering operation technique

Dušan Popov, Romeo Negrea, Miodrag Popov
Chin. Phys. B . 2016, 25(7): 070301 . **doi:** 10.1088/1674-1056/25/7/070301

Inverse problem of quadratic time-dependent Hamiltonians

Guo Guang-Jie, Meng Yan, Chang Hong, Duan Hui-Zeng, Di Bing
Chin. Phys. B . 2015, 24(8): 080301 . **doi:** 10.1088/1674-1056/24/8/080301

Unified treatment of the bound states of the Schiöberg and the Eckart potentials using Feynman path integral approach

A. Diaf
Chin. Phys. B . 2015, 24(2): 020302 . **doi:** 10.1088/1674-1056/24/2/020302

Transmission time in the reflectionless complex potential

Yin Cheng, Wang Xian-Ping, Shan Ming-Lei, Han Qing-Bang, Zhu Chang-Ping
Chin. Phys. B . 2014, 23(10): 100301 . **doi:** 10.1088/1674-1056/23/10/100301

Photon number cumulant expansion and generating function for photon added- and subtracted-two-mode squeezed states

Lu Dao-Ming, Fan Hong-Yi
Chin. Phys. B . 2014, 23(2): 020302 . **doi:** 10.1088/1674-1056/23/2/020302

The upper bound function of nonadiabatic dynamics in parametric driving quantum systems*

Lin Zhang(张林)† and Junpeng Liu(刘军鹏)

School of Physics and Information Technology, Shaanxi Normal University, Xi'an 710119, *China*

(Received 16 March 2019; revised manuscript received 29 May 2019; published online 25 July 2019)

The adiabatic control is a powerful technique for many practical applications in quantum state engineering, light-driven chemical reactions and geometrical quantum computations. This paper reveals a speed limit of nonadiabatic transition in a general time-dependent parametric quantum system that leads to an upper bound function which lays down an optimal criteria for the adiabatic controls. The upper bound function of transition rate between instantaneous eigenstates of a time-dependent system is determined by the power fluctuations of the system relative to the minimum gap between the instantaneous levels. In a parametric Hilbert space, the driving power corresponds to the quantum work done by the parametric force multiplying the parametric velocity along the parametric driving path. The general two-state time-dependent models are investigated as examples to calculate the bound functions in some general driving schemes with one and two driving parameters. The calculations show that the upper bound function provides a tighter real-time estimation of nonadiabatic transition and is closely dependent on the driving frequencies and the energy gap of the system. The deviations of the real phase from Berry phase on different closed paths are induced by the nonadiabatic transitions and can be efficiently controlled by the upper bound functions. When the upper bound is adiabatically controlled, the Berry phases of the electronic spin exhibit nonlinear step-like behaviors and it is closely related to topological structures of the complicated parametric paths on Bloch sphere.

Keywords: adiabatic dynamics, parametric driving, upper bound function

PACS: 03.65.Ca, 03.65.Ta, 03.65.Vf **DOI:** 10.1088/1674-1056/28/8/080301

1. Introduction

Quantum mechanics concerns more about equilibrium properties of a system by solving stationary Schrödinger equations to find intrinsic energy structures. It is a time-independent problem and many numerical methods have been developed such as the first principle calculation based on the density functional theory. However, in recent years, more attentions turn to quantum state control in order to manipulate quantum systems in a desired manner, guiding a quantum system evolving from an initial ground state to a target state through purposely designed parametric driving.[1]

The quantum control or engineering is definitely a time-dependent problem and needs real-time feedback for a practical application, for example, in the intermediate-state guiding chemical reactions (quantum catalysis)[2] or in the adiabatic quantum computations.[3] The time-dependent problems are more complicated than stationary ones because the system is non-conservative and will evolve to nonequilibrium states far-from-equilibrium dynamic,[4] which even disables an efficient description of the system because no quantum state can survive for such a quickly driving on the system.[5] Generally, not as that in the time-independent Hilbert space, an external driving always prevents the quantum system from keeping a complete basis because the Hilbert space is generally open. Traditionally, the main analytical method to deal with time-dependent problems is the perturbation theory, which holds a complete perturbed Hilbert space because the perturbation is weak. However, in many practical situations, the weak-driving condition fails and the perturbation method is invalid even in a very short driving time. But, fortunately, in most cases, the quantum control happens between two systems with different time scales, one is a classical driving system with relatively slow characteristic frequencies, and the other is the driven quantum one holding a fast intrinsic frequency determined by its internal levels. In this situation the adiabatic theory becomes a powerful tool and the adiabatic approximation is an important condition for the adiabatic dynamics. However, the normal condition of adiabatic approximation sometimes brings controversial results which, mainly, are derived from a rough static criterion.[6] Therefore, the adiabatic theorem should be carefully used because it is significant to design a robust strategy for coherent adiabatic control. As a strict condition for adiabatic approximation requires a very slow evolution of the quantum sate, fast adiabatic evolution[7] or shortcut adiabaticity[8] in order to overcome it are also presented.

Due to the above studies on time-dependent problems, in this paper, we will consider a general state evolution in a time-dependent parametric driving system. A speed limit of the state transition and a tighter condition for adiabatic approximation are found. The existence of an upper bound func-

*Project supported by the National Natural Science Foundation of China (Emergency Project, Grant Nos. 11447025 and 11847308).

†Corresponding author. E-mail: zhanglincn@snnu.edu.cn

© 2019 Chinese Physical Society and IOP Publishing Ltd

tion for nonadiabatic transition is related to the energy uncertainty on the speed of quantum evolution[9] and consistent with the trade-off between speed and cost in the shortcut to adiabaticity.[10] Our work reveals that the speed of nonadiabatic transition between instantaneous states is limited by the state power fluctuations relative to the minimum spectral gap of the system. Therefore, this real-time bound function can provide a necessary and sufficient condition for the adiabatic dynamics if the bound function is closely controlled by a feedback mechanism.[11] The calculations of this upper bound for adiabatic dynamics on Landau–Zener transition and electronic spin control are conducted in a general two-state time-dependent model. The adiabatic Berry phases along more complicated state loops in a high-dimensional driving parameter space are investigated.

2. Adiabatic evolution and non-adiabatic transitions

2.1. The quantum dynamics resolved by the instantaneous basis

Generally, a parametric driving quantum system can be described by the time-dependent Hamiltonian $\hat{H}(t)$, such as the following quadratic Hamiltonian[12,13]

$$\begin{aligned}\hat{H}(t) = & \frac{1}{2}\left[A(t)\hat{p}^2 + B(t)\hat{x}^2 + C(t)\left(\hat{x}\hat{p} + \hat{p}\hat{x}\right)\right] \\ & + D(t)\hat{p} + E(t)\hat{x} + F(t),\end{aligned} \tag{1}$$

where all the parameters $A(t)$, $B(t)$, …, $F(t)$ are continuous functions of time which can be used to describe the parametric driving or controlling of the quantum system. For a quantum state $|\Psi(t)\rangle$ of the above controlled system $\hat{H}(t)$, it evolves according to Schrödinger equation

$$\mathrm{i}\hbar\frac{\partial|\Psi(t)\rangle}{\partial t} = \hat{H}(t)|\Psi(t)\rangle, \tag{2}$$

starting from an initial state $|\Psi(0)\rangle$ to a final state of $|\Psi(\tau)\rangle$. The overall shift of the state $|\Psi(\tau)\rangle$ relative to the initial state can be described by an overlap

$$c(\tau) = \langle\Psi(0)|\Psi(\tau)\rangle = R(\tau)\mathrm{e}^{\mathrm{i}\alpha(\tau)},$$

where $0 \le R(\tau) \le 1$ and $\alpha \in [0, 2\pi)$. The change of $R(\tau)$ indicates a non-unitary state evolution, and the overall coherent phase $\alpha(\tau)$ accumulated during the evolution can be estimated by

$$\alpha(\tau) = \frac{1}{2i}\ln\frac{\langle\Psi(0)|\Psi(\tau)\rangle}{\langle\Psi(\tau)|\Psi(0)\rangle}, \tag{3}$$

which is contributed by both the state unitary evolution and the state transition process. The geometrical part of $\alpha(\tau)$ except for the dynamical part is called Pancharatnam phase (*P*-phase)[14] of a quantum wave.

If the Hamiltonian $\hat{H}(t)$ is Hermite, the unitary evolution keeps $R(t) = 1$, $t \in [0, \tau]$, no state transition occurs and the coherent phase Eq. (3) reduces to

$$\alpha(\tau) = \mathrm{Im}\ln\left[\langle\Psi(0)|\Psi(\tau)\rangle\right].$$

However, the detailed evolution of $R(t)$ and $\alpha(t)$ can not be resolved only by state overlap $c(\tau)$ because the state evolution in a time-dependent Hilbert space is irreversible ($[\hat{H}(t), \hat{H}(t')] \neq 0$) and the coherent phase α is closely dependent on the evolutionary trajectory of the state.

As the Hilbert space of a real parametric driving system is closed (the parameters now are real functions for the Hermitian property of $\hat{H}^\dagger = \hat{H}$), the system with time-dependent parameters admits a complete set of instantaneous eigenstates satisfying[15]

$$\hat{H}(t)|\varphi_n(t)\rangle = \varepsilon_n(t)|\varphi_n(t)\rangle, \tag{4}$$

and the instantaneous states hold

$$\langle\varphi_n(t)|\varphi_m(t)\rangle = \delta_{nm}; \sum_n |\varphi_n(t)\rangle\langle\varphi_n(t)| = 1 \tag{5}$$

for $n, m \in \mathbb{Z}$. With the above assumptions of instantaneous basis,[5] any transient state $|\Psi(t)\rangle$ of the system $\hat{H}(t)$ can be expanded by

$$|\Psi(t)\rangle = \sum_n a_n(t)\,\mathrm{e}^{\mathrm{i}\alpha_n(t)}|\varphi_n(t)\rangle, \tag{6}$$

and then the coherent phase of state $|\varphi_n(t)\rangle$ can be divided into two parts

$$\alpha_n(t) \equiv \theta_n(t) + \gamma_n(t), \tag{7}$$

where the first part

$$\theta_n(t) \equiv -\frac{1}{\hbar}\int_0^t \varepsilon_n(t')\,\mathrm{d}t' \tag{8}$$

is called the dynamical phase because it is accumulated from its energy $\varepsilon_n(t)$, and the second part

$$\gamma_n(t) \equiv \mathrm{i}\int_0^t \langle\varphi_n(t')|\dot{\varphi}_n(t')\rangle\,\mathrm{d}t' \tag{9}$$

is called the geometric P-phase rediscovered by Berry.[16]

By using Eq. (6), the transient energy of any state $|\Psi(t)\rangle$ is

$$E(t) = \sum_n |a_n(t)|^2\varepsilon_n(t) \equiv \sum_n p_n(t)\varepsilon_n(t), \tag{10}$$

with the initial energy being

$$E(0) = \sum_n p_n(0)\varepsilon_n(0). \tag{11}$$

Therefore, the energy change of the state $|\Psi(t)\rangle$ induced by the parametric driving is

$$\dot{E}(t) = \sum_n p_n(t)\dot{\varepsilon}_n(t) + \sum_n \dot{p}_n(t)\varepsilon_n(t), \tag{12}$$

which depends on two aspects: (i) the change of instantaneous energies of $\varepsilon_n(t)$, and (ii) the change of the population distribution of $p_n(t)$ in states $|\varphi_n(t)\rangle$. The energy change of the instantaneous eigenstates is

$$\dot{\varepsilon}_n(t) = \langle\varphi_n(t)|\dot{\hat{H}}(t)|\varphi_n(t)\rangle, \tag{13}$$

which is determined by the average driving power of $\dot{\hat{H}}$ in state $|\varphi_n(t)\rangle$, while the change of population distribution is determined by

$$\dot{a}_m(t) = -\sum_{n\neq m} \mathrm{e}^{\mathrm{i}[\alpha_n(t)-\alpha_m(t)]}\langle\varphi_m(t)|\dot{\varphi}_n(t)\rangle a_n(t). \tag{14}$$

We can see that the equivalence of Eq. (14) to Eq. (2) is supported by the validity of the transient expansion of Eq. (6) based on the assumptions of Eq. (4) and Eq. (5) for the parametric driving system.

2.2. The conventional adiabatic condition and the adiabatic states

Based on instantaneous basis, we can write Eq. (14) into another form of

$$\dot{a}_m(t) = -\sum_{n\neq m}\frac{\langle\varphi_m(t)|\dot{\hat{H}}(t)|\varphi_n(t)\rangle}{\varepsilon_n(t)-\varepsilon_m(t)}\mathrm{e}^{\mathrm{i}[\alpha_n(t)-\alpha_m(t)]}a_n(t). \tag{15}$$

Clearly, equation (15) describes the nonadiabatic state transition between instantaneous eigenstates. If the parametric driving is weak, equation (15) can be directly dropped if $\dot{a}_m(t) \ll 1$. This gives the conventional criterion for an adiabatic approximation[17] when

$$\sum_{n\neq m}\frac{\hbar}{|\varepsilon_n(t)-\varepsilon_m(t)|}\frac{\left|\langle\varphi_m(t)|\dot{\hat{H}}|\varphi_n(t)\rangle\right|}{|\varepsilon_n(t)-\varepsilon_m(t)|} \ll 1, \tag{16}$$

which is equivalent to

$$\hbar\sum_{n\neq m}\frac{|\langle\varphi_m(t)|\dot{\varphi}_n(t)\rangle|}{|\varepsilon_n(t)-\varepsilon_m(t)|} \ll 1.$$

The above condition actually means

$$|\langle\varphi_n(t)|\dot{\varphi}_m(t)\rangle| \ll |\langle\varphi_m(t)|\dot{\varphi}_m(t)\rangle|, \quad n\neq m, \tag{17}$$

which implies a very weak transition from one instantaneous state to other (transitionless quantum driving[18]). In a parameterized Hilbert space, adiabatic evolution corresponds to a parallel transportation of state vectors without any local rotations for phase accumulations. However, an overall rotation angle still be available because the parametric path is always confined to a manifold which has a geometrical curvature.

Then, if a state evolution is controlled by Eq. (16), after an evolution of time t, the state $|\Psi(t)\rangle$ should be very near to the adiabatic state

$$|\Psi(t)\rangle_{\mathrm{ad}} = \sum_n a_n(0)\,\mathrm{e}^{\mathrm{i}\alpha_n(t)}|\varphi_n(t)\rangle, \tag{18}$$

which is obtained by $\dot{a}_m(t) = 0$, $m = 1,2,\ldots$ from Eq. (6). Therefore, the energy of the adiabatic state is

$$E_{\mathrm{ad}}(t) \equiv \langle\hat{H}(t)\rangle_{\mathrm{ad}} = \sum_n p_n(0)\varepsilon_n(t). \tag{19}$$

Comparing the adiabatic energy $E_{\mathrm{ad}}(t)$ with Eq. (10), we can find that the energy change of an adiabatic process is only determined by the energy shifts of the instantaneous levels (an overall level shift or distortion of level profiles with respect to the system's parameters). The adiabatic evolution does not change the population distribution in the eigenstates $|\varphi_n(t)\rangle$ but only gives phase shifts to the initial states as Eq. (18). This implies that an adiabatic process is beyond any thermal process and keeps the population distribution unchanged. Adiabatic evolution displays a unitary evolution of a set of instantaneous eigenvectors of $\hat{H}(t)$ and only admits energy shifts following the driving parameters. That means no transition occurs during an adiabatic evolution and the level crossing (energy degenerate point) is not permitted during the adiabatic driving processes.[19]

As a reliable condition for the adiabatic approximation is a key for precise control on geometric phase, the conventional condition of Eq. (16) is weak and have been questioned by many authors such as in Ref. [20] because equation (16) only means $\dot{a}_m \ll 1$ but does not mean $\dot{a}_m = 0$. Therefore, the constant condition of $\dot{a}_m \ll 1$ to drop Eq. (15) leads to many conflict results when $\dot{a}_m$ changes with time and many improved approximate conditions were presented.[21] However, some new proposals are complicated to apply and lack of clean physical meanings. Here, we will discuss it physically to give a more general but tighter condition for the adiabatic control.

2.3. Upper bound functions for transition rates with energy gap

We can see that the conventional adiabatic condition of Eq. (16) is obtained by completely neglecting all the nonadiabatic terms in Eq. (15). Instead of dropping them, we use Cauchy–Schwarz inequality on Eq. (15) to find[22] (see Appendix B)

$$|\dot{a}_m(t)|^2 \leq \sum_{n\neq m}\left|\frac{\langle\varphi_m(t)|\dot{H}(t)|\varphi_n(t)\rangle}{\varepsilon_n(t)-\varepsilon_m(t)}\right|^2. \tag{20}$$

By using a simple notation $|\varphi_m(t)\rangle \to |m\rangle$, we can write the inequality by

$$|\dot{a}_m(t)|^2 \leq \sum_{n\neq m}\frac{\langle m|\dot{H}|n\rangle\langle n|\dot{H}|m\rangle}{\hbar^2\omega_{nm}^2(t)},$$

where the instantaneous transition frequencies are defined by

$$\omega_{nm}(t) = \frac{\varepsilon_n(t)-\varepsilon_m(t)}{\hbar}.$$

If the eigenenergy levels of the system keep crossing avoided during the quantum evolution (without level crossings) and the minimum level gap exists $\Delta_0 = \min_{m\neq n}|\varepsilon_m - \varepsilon_n|$, then we have $\hbar\omega_{nm}(t) \geq \Delta_0$ and

$$|\dot{a}_m(t)|^2 \leq \frac{1}{\Delta_0^2}\sum_{n\neq m}\langle m|\dot{H}|n\rangle\langle n|\dot{H}|m\rangle = \frac{1}{\Delta_0^2}\left[\langle m|\dot{H}^2|m\rangle - \langle m|\dot{H}|m\rangle^2\right]. \quad (21)$$

Equation (21) indicates that the magnitude of the non-adiabatic transition rate in any eigenstates $|\varphi_m\rangle$ must be smaller than the variance of energy changing. Certainly, this conclusion is based on an assumption of the minimum level gap existing during the evolution. However, the adiabatic theorem beyond a gap was also discussed in Ref. [23].

If we introduce a driving power operator of the system by the negative energy changing rate of the system

$$\hat{P}(t) = -\frac{\mathrm{d}}{\mathrm{d}t}\hat{H}(t),$$

then we can give an upper bound of non-adiabatic transition rate from eigenstate $|m\rangle$ by

$$|\dot{a}_m(t)|^2 \leq \frac{1}{\Delta_0^2}\left(\sqrt{\langle\hat{P}^2\rangle_m - \langle\hat{P}\rangle_m^2}\right)^2.$$

If the the power fluctuation in state $|m\rangle$ is defined by

$$\Delta P_m = \sqrt{\langle\hat{P}^2\rangle_m - \langle\hat{P}\rangle_m^2},$$

then, finally, we obtain the upper bound function for the non-adiabatic transition rate in state $|m\rangle$ as

$$|\dot{a}_m(t)| \leq \frac{\Delta P_m(t)}{\Delta_0} \equiv \Gamma_m(t). \quad (22)$$

The above real-time bound function $\Gamma_m(t)$ is actually a damping rate of $a_m(t)$ to estimate the non-adiabatic speed in a general quantum dynamics of parametric driving. The existence of the upper bound function $\Gamma_m(t)$ reveals that the transition rate from one instantaneous state to another is limited by the ratio between standard power fluctuation and the minimum level gap of the system. Or, reversely, the adiabatic approximation is valid only under the condition that the power fluctuations induced by the parametric driving is smaller than the minimum gap of the system. This real-time condition indicates that the non-adiabatic transition has a speed limit for a parametric driving system and the adiabatic process should be a slow evolution avoiding level mixing.

Based on Eq. (22), the probability amplitude in state $|m\rangle$ at time $t+\delta t$ can be estimated by

$$|a_m(t+\delta t)| \geq \mathrm{e}^{-\Gamma_m(t)\delta t}|a_m(t)|,$$

and the probability of remaining in state $|m\rangle$ during an adiabatic driving process (for a small $\Gamma_m(t)$) from an initial time t_i to a final time t_f can be roughly estimated by

$$p_m(t_\mathrm{f}) \geq \mathrm{e}^{-2\int_{t_\mathrm{i}}^{t_\mathrm{f}}\Gamma_m(t)\mathrm{d}t}p_m(t_\mathrm{i}). \quad (23)$$

3. The bound function in the driving parameter space

Considering N independent driving parameters $\lambda_j(t)$, $j = 1,2,\ldots N$, of a quantum system, the Hamiltonian can be written as $\hat{H}(t) = \hat{H}[\lambda_1(t),\cdots,\lambda_N(t)] \equiv \hat{H}(\boldsymbol{\lambda})$. At a quantum control time interval $t\in[0,T]$, the instantaneous eigenstates for $\hat{H}(\boldsymbol{\lambda})$ satisfy

$$\hat{H}(\boldsymbol{\lambda})|\varphi_n(\boldsymbol{\lambda})\rangle = \varepsilon_n(\boldsymbol{\lambda})|\varphi_n(\boldsymbol{\lambda})\rangle, \quad n = 1,2,\ldots.$$

Then any transient state $|\Psi(t)\rangle$ can be expanded by

$$|\Psi(t)\rangle = \sum_n a_n(t)\,|\varphi_n(\boldsymbol{\lambda})\rangle,$$

starting from an initial state $|\Psi(0)\rangle = \sum_n a_n(0)|\varphi_n(\boldsymbol{\lambda}_0)\rangle$, and the coefficients $a_n(t)$ of the transient state can be estimated by the bound function as

$$|\dot{a}_n(t)| \leq \frac{\Delta P_n(\lambda)}{\Delta_0} \equiv \Gamma_n(\lambda). \quad (24)$$

In the N-dimensional parameter space of $\boldsymbol{\lambda}$, a transient state of $\hat{H}(\boldsymbol{\lambda})$ corresponds to a point, and the power operator in the parametric Hilbert space is

$$\hat{P}(\lambda) = -\nabla_\lambda\hat{H}\cdot\dot{\boldsymbol{\lambda}}, \quad (25)$$

where $-\nabla_\lambda\hat{H}$ gives a gradient field of the system and $\dot{\boldsymbol{\lambda}}$ describes the dynamical equations of the parameters. If we define a general parametric force of the energy field and velocity in the parameter space as

$$\hat{\boldsymbol{F}}_\lambda = -\nabla_\lambda\hat{H}(\boldsymbol{\lambda}) = -\sum_{j=1}^{N}\frac{\partial\hat{H}}{\partial\lambda_j}\hat{\lambda}_j,$$

$$\boldsymbol{v}_\lambda = \dot{\boldsymbol{\lambda}} = \sum_{j=1}^{N}\frac{\mathrm{d}\lambda_j}{\mathrm{d}t}\hat{\lambda}_j,$$

respectively, where $\hat{\lambda}_j$ is the unit vector, then the power of Eq. (25) will be in a familiar form

$$\hat{P} = \hat{\boldsymbol{F}}_\lambda\cdot\boldsymbol{v}_\lambda, \quad (26)$$

which is the same as that defined in Ref. [24]. Alternatively, the above equation gives

$$\Delta E = \int\hat{P}\mathrm{d}t = \int_C\hat{\boldsymbol{F}}_\lambda\cdot\mathrm{d}\boldsymbol{\lambda}, \quad (27)$$

where ΔE is the energy change when the system evolves along a path C in the parameter space $\boldsymbol{\lambda}$. Clearly, if the field satisfies

$$\Delta E = \oint_C\hat{\boldsymbol{F}}_\lambda\cdot\mathrm{d}\boldsymbol{\lambda} = 0 \quad (28)$$

along any closed path, the field of the system $\hat{H}(\boldsymbol{\lambda})$ is conservative and has no singular point in the parameter space.

Therefore, if the parameters are controlled by the external driving, the bound Eq. (24) means that the non-adiabatic transition rates of the instantaneous eigenstates are limited by the fluctuations of "work" done by force $\boldsymbol{F}_\lambda$ per second when the state moves along the parametric driving path C. Basically, the force field of $\hat{H}(\boldsymbol{\lambda})$ is determined by the energy structure of the system and the path C depends on the solutions of the parametric equations $\dot{\boldsymbol{\lambda}}(t)$ due to the driving schemes.

Usually, a parametric driving Hamiltonian $\hat{H}(t)$ is solvable and it can be written in a form of

$$\hat{H}(t)=\hat{H}(\boldsymbol{\lambda})=\sum_{j=1}^{N}\lambda_j(t)\hat{L}_j, \tag{29}$$

where the operators $\{\hat{L}_1,\hat{L}_2,\ldots,\hat{L}_N\}$ can generate a finite M-dimensional Lie algebra by repeated commutations,

$$\left[\hat{L}_i,\hat{L}_j\right]=\mathrm{i}\hbar\sum_{k=1}^{M}\gamma_{ij}^{k}\hat{L}_k,$$

with $\gamma_{ij}^{k}=-\gamma_{ji}^{k}$. In most cases, the number of independent driving parameters satisfies $N\leq M$. Therefore, the driving parameters $\lambda_j(t)$ are piecewise continuous real functions defined on the control time interval. Surely, equation (29) is not unique and different parameterized form can be obtained by different Lie algebras defined on the diving system. Generally, the solutions of Eq. (29) can be obtained by the Lie transformation method.[13]

Further, if there exists a dynamical invariant for the above Hamiltonian $\hat{H}(t)$ in a form of[25]

$$\hat{I}(t)=\sum_{j=1}^{M}g_j(t)\hat{L}_j, \tag{30}$$

then a useful parameter space of $\boldsymbol{g}=(g_1,g_2,\ldots,g_M)$ can also be introduced and the continuous complex functions $g_j(t)$ at the same time interval will determined by the parametric equations of

$$\dot{g}_k(t)=\sum_{i,j=1}^{M}\lambda_i(t)\gamma_{ij}^{k}g_j(t). \tag{31}$$

If the parameter path $g_j(t)$ can be solved from Eq. (31), then the system has an invariant variable $\hat{I}(t)$ which can be used to discuss the adiabatic control by Lewis–Riesenfeld invariants method.[25,26] It is well known that the instantaneous eigenstates of $\hat{I}(t)$ provide an optimal basis to expand $|\Psi(t)\rangle$ by[8]

$$|\Psi(t)\rangle=\sum_n b_n(0)\,\mathrm{e}^{\mathrm{i}\beta_n(t)}\,|\phi_n(t)\rangle, \tag{32}$$

where

$$\beta_n(t)=\frac{1}{\hbar}\int_0^t\left\langle\phi_n\left(t'\right)\right|\mathrm{i}\hbar\frac{\partial}{\partial t'}-\hat{H}\left(t'\right)\left|\phi_n\left(t'\right)\right\rangle\mathrm{d}t'.$$

Compare Eq. (32) with Eq. (18), we can see a similar form of adiabatic state on this basis because the force field disappears in g-parameter space along the parametric path of Eq. (31) (the path is on a constant-energy surface). Therefore, a proper parameter space chosen to reveal the topological properties of Hamiltonian becomes important for an adiabatic control.

3.1. Bound functions for nonadiabatic transition in an avoided level crossing system with one driving parameter

Specifically, we consider a two-state system as an example, such as in a scheme of Landau–Zener transition shown in Fig. 1,[27] with only one driving parameter $\lambda(t)$,

$$\hat{H}(t)=\hbar\begin{pmatrix}\lambda(t) & \Omega_0\\ \Omega_0 & -\lambda(t)\end{pmatrix}, \tag{33}$$

where $\hbar\lambda(t)$ and $-\hbar\lambda(t)$ are the instantaneous energies of two bare states of $|e\rangle$ and $|g\rangle$, and Ω_0 is the coupling strength between them. Then the instantaneous eigenstates of Eq. (33) satisfy

$$\hat{H}(\lambda)\,|\varphi_\pm(\lambda)\rangle=\varepsilon_\pm(\lambda)\,|\varphi_\pm(\lambda)\rangle,$$

where the instantaneous energies are

$$\varepsilon_\pm(\lambda)=\pm\hbar\sqrt{\lambda^2(t)+\Omega_0^2},$$

and the instantaneous states are

$$|\varphi_+(\lambda)\rangle=\begin{pmatrix}\cos\theta(t)/2\\ \sin\theta(t)/2\end{pmatrix},\quad |\varphi_-(\lambda)\rangle=\begin{pmatrix}\sin\theta(t)/2\\ -\cos\theta(t)/2\end{pmatrix},$$

with

$$\cos\theta(t)=\frac{\lambda(t)}{\sqrt{\lambda^2(t)+\Omega_0^2}},\quad \sin\theta(t)=\frac{\Omega_0}{\sqrt{\lambda^2(t)+\Omega_0^2}}.$$

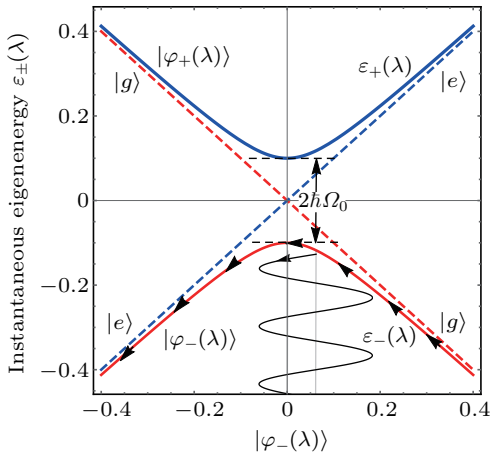


Fig. 1. The avoided crossing energies of two-level system controlled by only one driving parameter $\lambda(t)$. The dashed lines are the energies of bare states when the coupling rate Ω_0 is zero. Different sweeping processes enabled by the parametric setups are indicated by the arrows.

Here, we also introduce an instantaneous energy gap

$$\Delta(t) = \varepsilon_+(t) - \varepsilon_-(t) = 2\hbar\sqrt{\lambda^2(t) + \Omega_0^2}, \tag{34}$$

and we define $\Delta_0 = \min[\Delta(t)]$. Therefore, the nonadiabatic transition rates from states $|\varphi_\pm(\lambda)\rangle$ have a limit of

$$|\dot{a}_\pm(t)| \leq \frac{\Delta P_\pm(t)}{\Delta_0} \equiv \Gamma_\pm(t), \tag{35}$$

where the power operator of the parametric Hamiltonian is defined by

$$\hat{P}(t) \equiv -\dot{\hat{H}} = -\frac{\partial \hat{H}}{\partial \lambda}\dot{\lambda}(t).$$

3.1.1. Landau–Zener transition by linear sweeping driving

If the parameter $\lambda(t)$ enables a linear sweeping scheme as

$$\lambda(t) = \lambda_0 - \beta t,$$

where β is the chirp-rate of the driving field. The power operator

$$\hat{P}(t) = \hbar\beta \begin{pmatrix} 1 & 0 \\ 0 & -1 \end{pmatrix}$$

and its variance in state $|\varphi_-(\lambda)\rangle$ is

$$\Delta P_- = |\hbar\beta \sin\theta(t)| \leq |\hbar\beta|. \tag{36}$$

As shown in Fig. 1, the maximum nonadiabatic transition happens at the energy-level crossing point by $\partial\varepsilon_-(\lambda)/\partial\lambda = 0$ (at $\lambda = 0$) where the energy gap in this case is

$$\Delta(t) = 2\hbar\sqrt{(\lambda_0 - \beta t)^2 + \Omega_0^2},$$

and the minimum gap is $\Delta_0 = 2\hbar\Omega_0$. Then the bound function in this case for state $|\varphi_-(\lambda)\rangle$ is

$$|\dot{a}_-(t)| \leq \frac{\Delta P_-}{\Delta_0} = \frac{|\hbar\beta|}{\Delta(t)} \equiv \Gamma_-(t). \tag{37}$$

The above bound function reveals that the instantaneous transition rate is closely dependent on the energy gap and reaches the maximum value of $|\beta/2\Omega_0|$ at the energy-level crossing point ($\Delta(\lambda)/\mathrm{d}\lambda = 0$), which is often called the non-adiabatic point.

As the two-state system is closed, then

$$\langle\varphi_-|\left(\frac{\partial\hat{H}}{\partial\lambda}\right)^2|\varphi_-\rangle = |\langle\varphi_-|\frac{\partial\hat{H}}{\partial\lambda}|\varphi_+\rangle|^2 + \left(\frac{\partial\varepsilon_-}{\partial\lambda}\right)^2,$$

and the non-adiabatic bound $\Gamma_-(t)$ can be written as

$$|\dot{a}_-(t)| \leq \frac{|\dot{\lambda}(t)|}{\Delta_0}\left|\langle\varphi_-(\lambda)|\frac{\partial\hat{H}}{\partial\lambda}|\varphi_+(\lambda)\rangle\right|,$$

which, actually, is similar to the Fermi's golden rule. Therefore, the bound function gives Eq. (23) as

$$p_-(t_\mathrm{f}) \geq \exp\left[-2\int_{t_\mathrm{i}}^{t_\mathrm{f}}\Gamma_-(t)\,\mathrm{d}t\right]p_-(t_\mathrm{i}), \tag{38}$$

and which can be used to estimate the transition probability when $\Gamma_- \ll 1$. As the maximum transition rate from ground state $|\varphi_-(-\infty)\rangle = |g\rangle$ to upper state $|\varphi_+\rangle$ is $\Gamma_-(t)$, the probability remaining in the state $|\varphi_-\rangle$ after the parametric sweeping from right to left satisfies

$$p_-(\infty) \geq \exp\left[-\frac{1}{\Omega_0}\int_{-\infty}^{\infty}|\beta\sin\theta(t)|\,\mathrm{d}t\right] \approx \exp\left[-\frac{|\beta|}{2\Omega_0^2}\right], \tag{39}$$

which gives a lower probability in the state $|\varphi_-\rangle$ after a time interval of $1/2\Omega_0$ across the energy avoided crossing point. In Fig. 2, we exactly calculate the probabilities of $p_\pm(t) = |a_\pm(t)|^2$ (thick solid lines) as well as $p_{g,e}(t)$ (thin solid lines), where the bound probability of $p_\pm(\infty)$ determined by Eq.(39) and the Landau–Zener formula, $p_\mathrm{ZL} = \exp(-2\pi\Omega_0^2/2\beta)$, for $p_{g,e}(\infty)$ are also shown by the horizontal dashed lines. If $\beta/(2\Omega_0^2) \ll 1$, the system will keep an adiabatic evolution with a weak transition probability from the instantaneous state $|\varphi_-(t)\rangle$ to $|\varphi_+(t)\rangle$. As this model can be exactly solved, the upper bound function seems to be a bad estimation compared to the exact Landau–Zener formula,[28] but in a high dimensional parameter space, this bound will be a very useful tool for the real-time adiabatic control if an exact transition formula is absent.

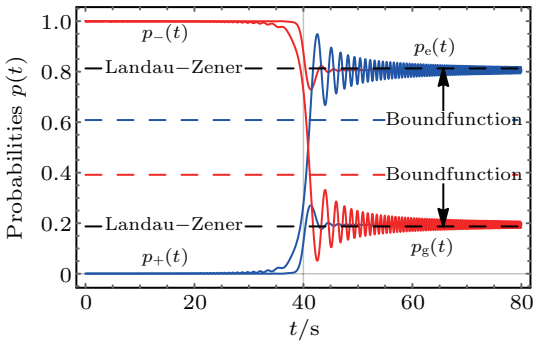


Fig. 2. The evolutions of the probabilities $p_\pm(t)$ (thick lines) in the instantaneous eigenstates of $|\varphi_\pm\rangle$ and $p_{e,g}(t)$ (thin lines) in the bare states of $|e,g\rangle$. The horizonal dashed lines are the probabilities predicted by the Landau–Zener formula and the upper bound determined by Eq. (39). The parameters are $\lambda_0 = 12$ Hz, $\beta = 0.3$ Hz/s, and $\Omega_0 = 0.4$ Hz.

3.1.2. Landau–Zener transition by back and forth sweeping driving

If the driving parameter gives a back and forth sweeping scheme as

$$\lambda(t) = \lambda_0 - \beta\sin(\omega t + \phi),$$

where $\beta > 0$ is the level sweeping amplitude around λ_0. The power operator in this case is

$$\hat{P}(t) = \hbar\beta\omega\begin{bmatrix}\cos(\omega t + \phi) & 0 \\ 0 & -\cos(\omega t + \phi)\end{bmatrix},$$

and its variance is

$$\Delta P_{-}=\frac{\hbar|\beta\omega\Omega_0\cos(\omega t+\phi)|}{\sqrt{\lambda^2(t)+\Omega_0^2}}\leq\hbar|\beta\omega|.$$

Therefore, the real-time bound function of the transition rate is

$$|\dot{a}_{-}(t)|\leq\frac{|\hbar\beta\omega\Omega_0|}{\sqrt{(\lambda_0-\beta)^2+\Omega_0^2}}\frac{|\cos(\omega t+\phi)|}{\Delta(t)}\equiv\Gamma_{-}(t),$$

and when $\beta<|\lambda_0|$ or $\beta>|\lambda_0|$, the bound function will be

$$|\dot{a}_{-}(t)|\leq\frac{|\hbar\beta\omega\cos(\omega t+\phi)|}{\Delta}(t)\equiv\Gamma_{-}(t).$$

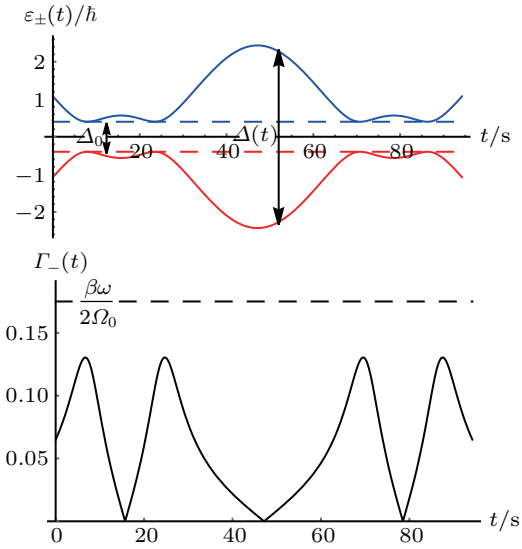


Fig. 3. The evolutions of the instantaneous energies $\varepsilon_{\pm}(t)$ of eigenstates $|\varphi_{\pm}\rangle$ and the bound function of $\Gamma_{-}(t)$. The parameters are $\lambda_0=12$ Hz, $\beta=1.4$ Hz, and $\Omega_0=0.4$ Hz.

Figure 3 demonstrates the transition bound $\Gamma_{-}(t)$ and reveals that the transition rate is closely dependent on the energy gap of the system and, for all the above cases, the bound function reveals a closer condition than the conventional adiabatic approximation of

$$\Gamma_{-}(t)\leq\left|\frac{\hbar\beta\omega}{\Delta_0}\right|=\left|\frac{\beta\omega}{2\Omega_0}\right|\ll1.$$

As there is no explicit analytical formula for transition probability in this case, the bound functions can give a rough transient estimation of the probability remaining in the state $|\varphi_{-}\rangle$

$$p_{-}(\delta t)\geq\mathrm{e}^{-2\Gamma_{-}(t)\delta t}p_{-}(0)\approx\exp\left(-\left|\frac{\beta\omega}{2\Omega_0}\right|\delta t\right),\quad(40)$$

when the system starts from the ground state for $p_{-}(0)=1$. Surely, this probability is a very bad prediction for a longtime evolution, but the bound function $\Gamma(t)$ can provide a better real-time estimation of the non-adiabatic transition rate for a robust feed-back adiabatic control during transitionless quantum driving for time-dependent quantum systems.

3.2. Adiabatic control of spin by the sweeping magnetic fields

Now, let us calculate the upper bound function with more driving parameters in the two-state system with a general form of

$$\hat{H}(t)=\hbar\begin{bmatrix}\Delta(t) & \Omega^*(t)\\ \Omega(t) & -\Delta(t)\end{bmatrix}.$$

The Hamiltonian can be expressed by Pauli operators $\{\hat{\sigma}_x,\hat{\sigma}_y,\hat{\sigma}_z\}$ in a form of Eq. (29)

$$\hat{H}(t)=\hbar\Delta(t)\hat{\sigma}_z+\hbar\Omega^*(t)\hat{\sigma}_{+}+\hbar\Omega(t)\hat{\sigma}_{-},$$

where $\hat{\sigma}_{\pm}=(\hat{\sigma}_x\pm\mathrm{i}\hat{\sigma}_y)/2$ and the parameters $\Delta(t)$ and $\Omega(t)$ can be any time-dependent functions for different driving schemes in a practical control process.

A typical application of the above model is for spin qubit control with a varying magnetic field shown in Fig. 4. The driving magnetic field is usually constructed by superposition of two varying magnetic fields, one is $\boldsymbol{B}_{\parallel}$ along z direction and the other $\boldsymbol{B}_{\perp}$ is perpendicular to $\boldsymbol{B}_{\parallel}$ and rotates with a frequency of ω.[16] The combined magnetic field $\boldsymbol{B}(t)$ can be generally described by

$$\begin{aligned}B_x(t)&=B_0(t)\sin[\alpha(t)]\cos(\omega t),\\ B_y(t)&=B_0(t)\sin[\alpha(t)]\sin(\omega t),\\ B_z(t)&=B_0(t)\cos[\alpha(t)],\end{aligned}\quad(41)$$

where the magnitude of $\boldsymbol{B}(t)$ is $B_0(t)$ and $\alpha(t)$ is the instaneous angle of the sweeping cone. The spin Hamiltonian $\hat{H}=\frac{e}{m}\boldsymbol{B}(t)\cdot\hat{\boldsymbol{S}}$ reads

$$\hat{H}(t)=\frac{\hbar\omega_0(t)}{2}\begin{bmatrix}\cos\alpha(t) & \sin\alpha(t)\,\mathrm{e}^{-\mathrm{i}\omega t}\\ \sin\alpha(t)\,\mathrm{e}^{\mathrm{i}\omega t} & -\cos\alpha(t)\end{bmatrix},\quad(42)$$

where the Lamor frequency of electron spin is

$$\omega_0(t)=\frac{eB_0(t)}{m}.\quad(43)$$

As the sweeping magnetic field $\boldsymbol{B}(t)$ can be denoted by a spherical coordinate: $\boldsymbol{B}(t)\equiv(B_0(t),\alpha(t),\omega t)$, we can introduce three spherical driving parameters as

$$\begin{aligned}\lambda_1(t)&=eB_0(t)/m\equiv\omega_0(t),\\ \lambda_2(t)&=\alpha(t),\\ \lambda_3(t)&=\omega t,\end{aligned}\quad(44)$$

then the Hamiltonian of Eq. (42) is put into a form of

$$\hat{H}(\lambda_1,\lambda_2,\lambda_3)=\frac{\hbar\lambda_1}{2}\begin{bmatrix}\cos\lambda_2 & \sin\lambda_2\,\mathrm{e}^{-\mathrm{i}\lambda_3}\\ \sin\lambda_2\,\mathrm{e}^{\mathrm{i}\lambda_3} & -\cos\lambda_2\end{bmatrix},\quad(45)$$

which is defined in λ-parameter space. Alternatively, another popular parameterized form,

$$\hat{H}(u,v,w)=u(t)\hat{\sigma}_x+v(t)\hat{\sigma}_y+w(t)\hat{\sigma}_z,$$

is often used to define a generalized Bloch sphere where the new parameters are defined by

$$u(t)=\frac{\hbar}{2}\lambda_1(t)\sin[\lambda_2(t)]\cos[\lambda_3(t)],$$
$$v(t)=\frac{\hbar}{2}\lambda_1(t)\sin[\lambda_2(t)]\sin[\lambda_3(t)],$$
$$w(t)=\frac{\hbar}{2}\lambda_1(t)\cos[\lambda_2(t)], \tag{46}$$

and we can easily find that the Bloch parameters $u(t)$, $v(t)$, and $w(t)$ satisfy

$$u^2(t)+v^2(t)+w^2(t)=\frac{\hbar^2}{4}\lambda_1^2(t).$$

It is well known that the spin operators $\{\hat{\sigma}_x,\hat{\sigma}_y,\hat{\sigma}_z\}$ construct a SU(2) Lie algebra and the instantaneous spin eigenstates and eigenvalues are

$$|\varphi_+(t)\rangle=\begin{pmatrix}\cos\dfrac{\lambda_2(t)}{2}\\ \sin\dfrac{\lambda_2(t)}{2}e^{i\lambda_3(t)}\end{pmatrix},\quad \varepsilon_+=+\frac{1}{2}\hbar\lambda_1(t),$$
$$|\varphi_-(t)\rangle=\begin{pmatrix}\sin\dfrac{\lambda_2(t)}{2}e^{-i\lambda_3(t)}\\ -\cos\dfrac{\lambda_2(t)}{2}\end{pmatrix},\quad \varepsilon_-=-\frac{1}{2}\hbar\lambda_1(t),$$

which gives an energy gap of $\Delta(t)=\hbar\lambda_1(t)$.

The instantaneous eigenstates $|\varphi_+(t)\rangle$ and $|\varphi_-(t)\rangle$ represent the spin-up and spin-down states with respect to the transient direction of the magnetic field $\boldsymbol{B}(t)$, respectively. As spin states $|\varphi_\pm(t)\rangle$ follow the direction of $\boldsymbol{B}(t)$ controlled by the driving parameters $\lambda_1(t)$, $\lambda_2(t)$, and $\lambda_3(t)$, the physical conditions for a practical spin control satisfy $\lambda_1\gg\dot{\lambda}_2,\dot{\lambda}_3$ (or $\omega_0\gg\dot{\alpha},\omega$) because the internal Lamor frequency of electronic spin ($\omega_0\approx1.759\times10^{11}B_0$) is much larger than the varying speed of the classical driving parameters.

The general spin state $\Psi(t)$ can then be expanded by

$$\Psi(t)=a_-(t)\,e^{i\theta_-(t)}|\varphi_-(t)\rangle+a_+(t)\,e^{i\theta_+(t)}|\varphi_+(t)\rangle, \tag{47}$$

where the dynamical phases are

$$\theta_\pm(t)\equiv\mp\frac{1}{2}\int_0^t\lambda_1(t')\mathrm{d}t'.$$

In this case, the dynamical equations for the transition rates are

$$\dot{a}_+(t)=-a_-(t)\frac{\langle\varphi_+(t)|\dot{H}(t)|\varphi_-(t)\rangle}{\varepsilon_--\varepsilon_+}e^{i\int_0^t\lambda_1(t')\mathrm{d}t'}-a_+(t)\langle\varphi_+(t)|\dot{\varphi}_+(t)\rangle, \tag{48}$$
$$\dot{a}_-(t)=-a_+(t)\frac{\langle\varphi_-(t)|\dot{H}(t)|\varphi_+(t)\rangle}{\varepsilon_+-\varepsilon_-}e^{-i\int_0^t\lambda_1(t')\mathrm{d}t'}-a_-(t)\langle\varphi_-(t)|\dot{\varphi}_-(t)\rangle, \tag{49}$$

and the transient power operator $\hat{P}(t)$ of Hamiltonian Eq. (42) with parameters $\boldsymbol{\lambda}=(\lambda_1,\lambda_2,\lambda_3)$ reads

$$\hat{P}(t)\equiv-\dot{\hat{H}}(\boldsymbol{\lambda},\dot{\boldsymbol{\lambda}})=\frac{\hbar}{2}\begin{bmatrix}\dot{\lambda}_1\cos\lambda_2-\lambda_1\dot{\lambda}_2\sin\lambda_2 & \left[(\dot{\lambda}_1-i\lambda_1\dot{\lambda}_3)\sin\lambda_2+\lambda_1\dot{\lambda}_2\cos\lambda_2\right]e^{-i\lambda_3}\\ \left[(\dot{\lambda}_1+i\lambda_1\dot{\lambda}_3)\sin\lambda_2+\lambda_1\dot{\lambda}_2\cos\lambda_2\right]e^{i\lambda_3} & -\dot{\lambda}_1\cos\lambda_2+\lambda_1\dot{\lambda}_2\sin\lambda_2\end{bmatrix}. \tag{50}$$

We can easily verify that equation (50) satisfies Eq. (26) and the parametric path is determined by the driving scheme of Eq. (44). Therefore, the upper bound for non-adiabatic transition rate in this case can be estimated by Eq. (24) in details if the time-dependent functions of the driving parameters are given. In the following sections, the bound functions of adiabatic control with two different driving schemes are calculated and the geometric phases for the adiabatic spin dynamics are investigated.

3.2.1. Magnetic field sweeping in the azimuthal direction

A magnetic field sweeping in the azimuthal direction with a fixed polar angle α is a conventional scheme to drive electronic spins, which is realized by the driving parameters of $\lambda_1(t)=eB_0/m=\omega_0$, $\lambda_2(t)=\alpha$, and $\lambda_3(t)=\omega t$ (see Fig. 4), and the transition dynamics for this control scheme will be

$$\dot{a}_+=-i\omega\sin^2\frac{\alpha}{2}a_++\frac{i\omega\sin\alpha}{2}e^{i\delta t}a_-, \tag{51}$$

$$\dot{a}_-=i\omega\sin^2\frac{\alpha}{2}a_-+\frac{i\omega\sin\alpha}{2}e^{-i\delta t}a_+, \tag{52}$$

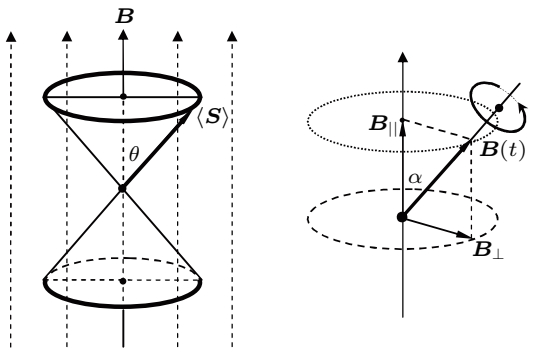


Fig. 4. The control of electronic instantaneous spin states by (a) a magnetic field in z direction and (b) a sweeping magnetic field denoted by spherical coordinates of $\boldsymbol{B}(t)$.

where the detuning $\delta=\omega_0-\omega$. Consequently, the power operator reduces to

$$\hat{P}(t)=\frac{\hbar}{2}\omega_0\begin{bmatrix}0 & -i(\omega\sin\alpha)e^{-i\omega t}\\ i(\omega\sin\alpha)e^{i\omega t} & 0\end{bmatrix},$$

and the upper bound for non-adiabatic transition rates calculated by Eq. (24) are

$$|\dot{a}_{\pm}| \leq \left| \left(\frac{1}{2}\right) \omega \sin\alpha \right| \equiv \Gamma,$$

which can also be directly obtained from Eqs. (51) and (52), leading to a convectional adiabatic condition of adiabatic control for $\Gamma \ll 1$. When the spin is initially in spin-down state, the probability estimation of Eq. (23) on spin-up state at a later time $t \ll 1$ will be checked by the strict solution of

$$p_{+}(t) = |a_{+}(t)|^2 = \frac{\omega^2 \sin^2\alpha}{\Omega^2} \sin^2\left(\frac{\Omega}{2}t\right), \tag{53}$$

where the effective flip frequency is

$$\Omega = \sqrt{(\omega_0 - \omega\cos\alpha)^2 + (\omega\sin\alpha)^2},$$

and equation (23) gives

$$p_{+}(t) \approx \left(\frac{1}{2}\omega\sin\alpha\right)^2 t^2,$$

which is exactly the expansion of Eq. (53) at a very short time $t \ll 1$. As the rigorous solution of this case is well studied,[15] the geometric phase in this case is omitted.

3.2.2. Magnetic field sweeping in both azimuthal and polar directions

Now we would like to consider a more general controlling magnetic field for $\dot{\lambda}_1(t) = 0$, $\dot{\lambda}_2 = \dot{\alpha}(t)$, and $\dot{\lambda}_3 = \omega$, then the driving power operator of the system is

$$\hat{P}(t) \equiv -\dot{\hat{H}}(t) = \frac{\hbar\omega_0}{2} \times \begin{bmatrix} -\dot{\alpha}\sin\alpha & (\dot{\alpha}\cos\alpha - \mathrm{i}\omega\sin\alpha)\,\mathrm{e}^{-\mathrm{i}\omega t} \\ (\dot{\alpha}\cos\alpha + \mathrm{i}\omega\sin\alpha)\,\mathrm{e}^{\mathrm{i}\omega t} & \dot{\alpha}\sin\alpha \end{bmatrix},$$

and the transition dynamics for this control scheme are

$$\dot{a}_{+} = -\mathrm{i}\omega\sin^2\frac{\alpha}{2}a_{+} + \frac{\mathrm{i}\omega\sin\alpha - \dot{\alpha}}{2}\mathrm{e}^{\mathrm{i}\delta t}a_{-}, \tag{54}$$

$$\dot{a}_{-} = \mathrm{i}\omega\sin^2\frac{\alpha}{2}a_{-} + \frac{\mathrm{i}\omega\sin\alpha + \dot{\alpha}}{2}\mathrm{e}^{-\mathrm{i}\delta t}a_{+}. \tag{55}$$

The upper bound function of this control scheme becomes

$$|\dot{a}_{\pm}(t)| \leq \frac{1}{2}\sqrt{[\dot{\alpha}(t)]^2 + [\omega\sin\alpha(t)]^2} \equiv \Gamma_{\pm}(t), \tag{56}$$

which sets the modulus bound for the changing rates of both driving parameters as shown in Fig. 5. When both the changing rates $\dot{\alpha}/\omega_0$ and ω/ω_0 keep small, the dynamics will conduct an adiabatic evolution which leads to an adiabatic geometric phases for $|\varphi_{\pm}\rangle$ as

$$\gamma_{\pm}(t) = \mathrm{i}\int_0^t \langle\varphi_{\pm}|\dot{\varphi}_{\pm}\rangle\,\mathrm{d}\tau = \mp\omega\int_0^t \sin^2\left[\frac{\alpha(\tau)}{2}\right]\mathrm{d}\tau. \tag{57}$$

Specifically, if the polar angle of $\alpha(t)$ is controlled by a periodic function of

$$\alpha(t) = \alpha_0 + \alpha_1\sin(\nu t),$$

the upper bound function for the adiabatic control reads

$$\Gamma(t) = \frac{1}{2}\sqrt{\omega^2\sin^2[\alpha_0 + \alpha_1\sin(\nu t)] + \nu^2\alpha_1^2\cos^2(\nu t)}.$$

The dynamics of transition rates $|\dot{a}_{\pm}(t)|$ and the bound function are both shown in Fig. 5 for different driving parameters. The bound function exhibits a good real-time constraint on the transition rate and reveals that low sweeping frequencies (ω and ν) and small sweeping amplitude α_1 are critical for an adiabatic state evolution.

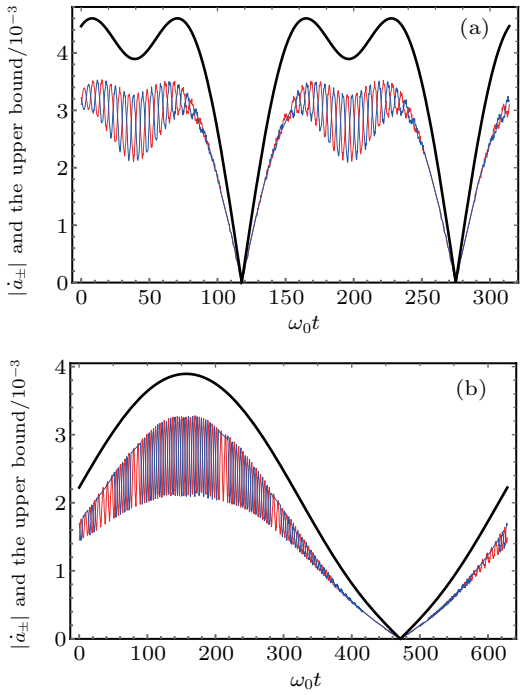


Fig. 5. The evolutions of the transition rate $|\dot{a}_{+}(t)|$ (red thin lines), $|\dot{a}_{-}(t)|$ (blue thin lines) and their upper bound functions $\Gamma(t)$ (black lines). The control parameters are $\alpha_0 = 0.2$, $\alpha_1 = 0.2$, $\omega = 0.02\omega_0$, (a) $\nu = 0.04\omega_0$ and (b) $\nu = 0.01\omega_0$, with the initial probabilities $p_{\pm}(0) = 0.5$.

For an adiabatic case of $\Gamma(t) \leq \sqrt{\omega^2 + \nu^2\alpha_1^2}/2 \ll 1$, the adiabatic geometric phase along a parametric path will be strictly calculated by

$$\gamma_{\pm}(t) = \pm\frac{1}{2}\omega\left[\mathrm{J}_0(\alpha_1)\cos\alpha_0 - 1\right]t \pm \omega\sum_{n\neq 0}\mathrm{J}_n(\alpha_1)\frac{\cos(\alpha_0 + n\nu t/2)\sin(n\nu t/2)}{n\nu}, \tag{58}$$

where $\mathrm{J}_n(z)$ is the Bessel function of the first kind, α_0 is the

initial polar angle, α_1 and ν are the sway amplitude and frequency of the driving magnetic filed $\boldsymbol{B}(t)$ along the polar direction. Figure 6 compares the dynamics of strict phases with the geometric phases of $\gamma_-(t)$ for the instantaneous spin-down state $\varphi_-(t)$ under different frequency ratios ν/ω and α_1/α_0. The strict calculations on Eqs. (54) and (55) (the thin blue lines) verify that equation (58) is a very good result when the bound function keeps small. However, if the parametric driving breaks the requirement of a small bound function, equation (58) becomes inaccurate and the real phase of $a_-(t)$ will deviate from Eq. (58) with irregular oscillations due to the non-adiabatic state transitions.

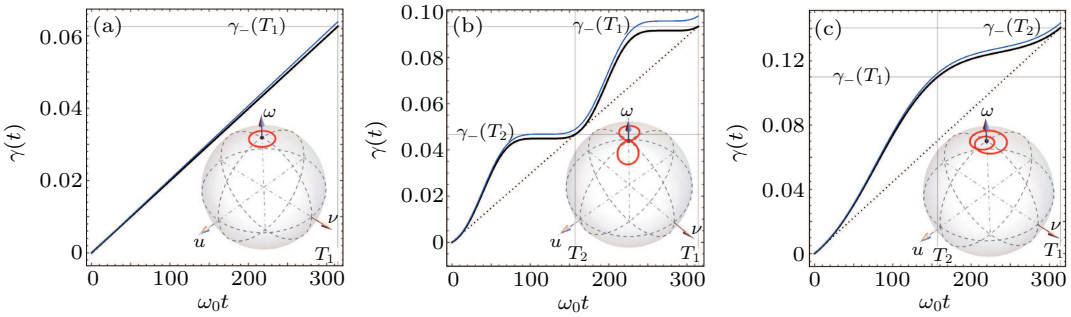


Fig. 6. The geometric phases $\gamma_-(t)$ for instantaneous eigenstate $|\varphi_-\rangle$ under different driving parameters. The thick black solid lines are the analytical solutions of Eq. (58), the thin blue lines are the real phases calculated by Eqs. (54) and (55), the black dotted diagonal lines are the first term of Eq. (58) and the horizonal lines are labeled by Eq. (59) in different driving periods. Insets: the parametric paths of three different driving schemes in the Bloch space, and all the driving paths are counterclockwise. The driving parameters are $\omega = 0.02\omega_0$, (a) $\alpha_0 = 0.2$, $\alpha_1 = 0$; (b) $\omega/\nu = 1/2$, $\alpha_0 = 0.2$, $\alpha_1 = 0.2$; and (c) $\omega/\nu = 2/1$, $\alpha_0 = 0.2$, $\alpha_1 = 0.1$.

The dynamics of the nonlinear geometric phase in an adiabatic process can be divided into two different parts: the linear part which increases linearly with time (the dotted lines in Figs. 6(b) and 6(c)) and the nonlinear part which induced by the parametric oscillation in the polar direction. The adiabatic geometric phases related to two periods of $T_1 = 2\pi/\omega$ and $T_2 = 2\pi/\nu$ are

$$\gamma_\pm(T_i) = \pm\frac{1}{2}\left[\mathrm{J}_0(\alpha_1)\cos\alpha_0 - 1\right]\omega T_i, \tag{59}$$

which are displayed in Fig. 6 by the grey horizontal grid lines just for references. Clearly, in a conventional case of $\alpha_1 = 0$, equation (58) gives the familiar Berry phase in a cyclic period of $T = 2\pi/\omega$ with a solid angle of $\pm\pi(\cos\alpha_0 - 1)$, deriving only from the linear part of Eq. (58) (see Fig. 6(a)). However, for a control period of $T = 2\pi/\nu$ along a closed parametric path for $\alpha_1 \neq 0$, the invariant Berry phase will be

$$\gamma_\pm(2\pi/\nu) = \pm\pi\frac{\omega}{\nu}\left[\mathrm{J}_0(\alpha_1)\cos\alpha_0 - 1\right]. \tag{60}$$

As we have two control frequencies, ω and ν, along the azimuthal and polar directions, respectively, there exist two evolutionary periods of T for $\hat{H}(t+T) = \hat{H}(t)$ that will lead to rich geometric structures of the Lissajous parametric paths on Bloch sphere determined by the frequency ratio of ν/ω and the amplitude ratio of α_1/α_0 (see Fig. 7). Therefore, the Berry phase in this case should be determined by a common period covering a closed path in the parameter space.

For the adiabatic dynamics, when the driving ratio ω/ν is a rational number, that is $\omega/\nu = p/q$, where $p, q \in \mathbb{N}$, the common period is $T = pT_1 = qT_2$ while the adiabatic geometric phase is $\gamma_\pm(T) = \pm p\pi[\mathrm{J}_0(\alpha_1)\cos\alpha_0 - 1]$. For $\alpha_1/\alpha_0 < 1$, the path has a simple form and does not intersect with itself. But for $\alpha_1/\alpha_0 \geq 1$, the orbit intersects with itself and the region S covered by the path on the Bloch sphere will be divided into different overlapped areas and each area enclosed by a loop contributes its respective part because the total covering area is the sum of them. This is due to

$$\gamma_\pm(t) = \mp\oint_C \sin^2\frac{\alpha}{2}\mathrm{d}\phi = \mp\frac{1}{2}\int_S \sin\alpha\cdot\mathrm{d}S, \tag{61}$$

where $\phi = \omega t$ is the azimuthal angle of the path C on the Bloch sphere and $\mathrm{d}S$ is the area element of the region S covered by the path. Equation (61) reveals a $\sin\alpha$-weighted area contribution to the geometric phase. That means when the polar angle α is constant ($\alpha_1 = 0$), the state $|\varphi_-(t)\rangle$ evolves along a circle path on the Bloch sphere and its geometric phase increases linearly with a slope proportional to $\sin\alpha$ as shown in Fig. 6(a). Figure 6(b) demonstrates that, for a case of $\omega/\nu = 1/2$ and $\alpha_1/\alpha_0 = 1$, the path has a knot shape and the region S is divided into two separated areas by one intersection point (one vertex). Therefore the phases exhibit a two step-like dynamics during the command period of $T = T_1$. While, for $\omega/\nu = 2/1$ and $\alpha_1/\alpha_0 < 1$, figure 6(c) shows that the region S consists of two overlapped areas, which leads to a different phase dynamics with only one step during the command period of $T = T_2$. The areas enclosed by more loops formed by the complicated periodic paths are shown in Fig. 7 and the parametric path has a close relation to a Eulerian path in a view of graph theory. However, when the ratio ω/ν is an irrational number, no closed path can be found in the parameter space to fulfill $\hat{H}(t+T) = \hat{H}(t)$ and no invariant Berry phase exists in this case because the parametric path does not enclose an area (no enclosed boundary).

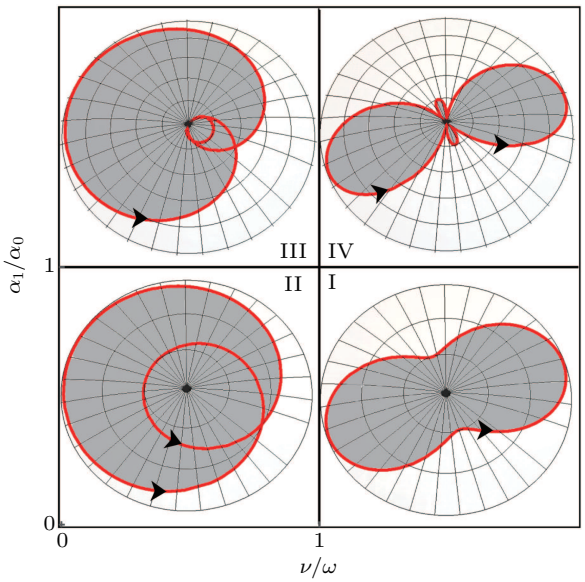


Fig. 7. The parametric paths of different driving schemes in the parameter space of Bloch sphere. The driving parameters are $\omega = 0.02\omega_0$, $\alpha_0 = 0.2$, (I) $\nu/\omega = 1/2$, $\alpha_1/\alpha_0 = 1/2$; (II) $\nu/\omega = 2/1$, $\alpha_1/\alpha_0 = 1/2$; (III) $\nu/\omega = 1/2$, $\alpha_1/\alpha_0 = 3/2$; and (IV) $\nu/\omega = 2/1$, $\alpha_1/\alpha_0 = 3/2$.

Therefore, the above analysis indicates that the phase evolution of a quantum state is closely associated with the geometric structure of its evolutionary path in the parameter space. Above all, the topological property of the Berry phase can be perfectly controlled by the parametric paths through a designed parametric driving under the control of the time-dependent bound function proposed in this paper.

Appendix A: The proof of Eq. (20)

The Cauchy's inequality reads

$$\left|\sum_{j=1}^{n} x_j y_j\right|^2 \leq \sum_{j=1}^{n} |x_j|^2 \sum_{j=1}^{n} |y_j|^2,$$

where x_j and y_j are arbitrary complex numbers. Therefore, according to Eq. (15), we have

$$|\dot{a}_m(t)|^2 \leq \sum_{n\neq m} \left|\frac{\langle\varphi_m(t)|\dot{H}(t)|\varphi_n(t)\rangle}{\varepsilon_n(t)-\varepsilon_m(t)}\right|^2 \sum_{n\neq m} |a_n(t)|^2$$

$$\leq \sum_{n\neq m} \left|\frac{\langle\varphi_m(t)|\dot{H}(t)|\varphi_n(t)\rangle}{\varepsilon_n(t)-\varepsilon_m(t)}\right|^2,$$

where we have used

$$\sum_{n\neq m} |a_n(t)|^2 \leq \sum_{n} |a_n(t)|^2 = 1.$$

References

[1] Dong D and Petersen I R 2010 *IET Control Theory and Appl.* **4** 2651
[2] Ospelkaus S, Ni K K, Wang D, de Miranda M H G, Neyenhuis B, Quéméner G, Julienne P S, Bohn J L, Jin D S and Ye J 2010 *Science* **327** 853
[3] Albash T and Lidar D A 2018 *Rev. Mod. Phys.* **90** 015002
[4] Eisert J, Friesdorf M and Gogolin C 2015 *Nat. Phys.* **11** 124
[5] Deffner S and Lutz E 2013 *Phys. Rev. Lett.* **111** 010402
[6] Marzlin K P and Sanders B C 2004 *Phys. Rev. Lett.* **93** 160408
[7] Petiziol F, Dive B, Mintert F and Wimberger S 2018 *Phys. Rev. A* **98** 043436
[8] Torrontegui E, Ibáñez S, Martínez-Garaot S, Modugno M, del Campo A, Guéry-Odelin D, Ruschhaupt A, Chen X and Muga J G 2013 *Adv. At. Mol. Opt. Phys.* **62** 117
[9] Pfeifer P 1993 *Phys. Rev. Lett.* **70** 3365
[10] Campbell S and Deffner S 2017 *Phys. Rev. Lett.* **118** 100601
[11] Tong D M 2010 *Phys. Rev. Lett.* **104** 120401
[12] Choi J R and Nahm I H 2007 *Int. J. Theor. Phys.* **46** 1
[13] Zhang L and Zhang W P 2016 *Ann. Phys.* **373** 424
[14] Pancharatnam S 1956 *Proc. Indian Acad. Sci. A* **44** 247
[15] Griffiths D J 2005 *Introduction to Quantum Mechanics*, 2nd edn. (Upper Saddle River: Pearson Prentice Hall)
[16] Berry M V 1984 *Proc. R. Soc. Lond. A* **392** 45
[17] Aguiar Pinto A, Nemes M, Peixoto de Faria J and Thomaz M T 2000 *Am. J. Phys.* **68** 955
[18] Berry M V 2009 *J. Phys. A: Math. Theor.* **42** 365303
[19] Sarandy M S and Lidar D A 2005 *Phys. Rev. A* **71** 012331
[20] Du J F, Hu L Z, Wang Y, Wu J D, Zhao M S and Suter D 2008 *Phys. Rev. Lett.* **101** 060403
[21] Comparat D 2009 *Phys. Rev. A* **80** 012106
[22] Cao H X, Guo Z H, Chen Z L and Wang W H 2013 *Sci. China-Phys. Mech. Astron.* **56** 1401
[23] Avron J E and Elgart A 1999 *Commun. Math. Phys.* **203** 445
[24] Venkatesh B P, Watanabe G and Talkner P 2015 *New J. Phys.* **17** 075018
[25] Lewis H R Jr and Riesenfeld W B 1969 *J. Math. Phys.* **10** 1458
[26] Chen X, Ruschhaupt A, Schmidt S, del Campo A, Guéry-Odelin D and Muga J G 2010 *Phys. Rev. Lett.* **104** 063002
[27] Shevchenko S N, Ashhab S and Nori F 2010 *Phys. Rep.* **492** 1
[28] Wittig C 2005 *J. Phys. Chem. B* **109** 8428